GSA Data Repository Item 2017399
Griffis, N.P., Mundil, R., Montañez, I.P., Isbell, J., Fedorchuk, N., Vesely F., Iannuzzi, R., and Yin, Q.-Z., 2017, A new stratigraphic framework built on U-Pb single-zircon TIMS ages and implications for the timing of the penultimate icehouse (Paraná Basin, Brazil): GSA Bulletin, https://doi.org/10.1130/B31775.1.

Data Supplement

PREVIOUS U-PB ANALYSIS AND BIOSTRATIGRAPHY

Candiota Coal Interval

Candiota A (LoCan1) (*Locality 31°27'43.69"S 53°41'33.01"W*)

De Matos et al. (2001) presented the first radioisotopic U-Pb age for zircons extracted from Paraná Basin coal deposits. A lower intercept concordia age of 267 ±3.4 Ma (Mean Square Weight Deviation (MSWD) = 0.31 of concordance; σ not specified) for the lowermost Candiota tonstein A was calculated using four discordant zircon results obtained by multi-crystal batch TIMS analysis (Fig. 1). This result cannot be further evaluated as the uncertainties of the individual ages and isotopic data are not published. Guerra-Sommer et al. (2008a) reanalyzed this tonstein by TIMS and obtained a weighted mean age of 296 ±4.2 Ma (2σ) based on two multi-crystal batch analyses and concluded that the zircons analyzed by de Matos et al. (2001) suffered from Pb-loss (Fig 1). The age reported by de Matos et al. (2001) is a lower intercept age. Therefore if recent Pb-loss occurred then the upper intercept age (867 Ma) should reflect the age of crystallization. Additionally, the reported weighted mean age (Guerra-Sommer et al., 2008a) is calculated from four discordant analyses. A fifth batch analysis is concordant and yields an age of 300.8 ±3.4 Ma, however it was excluded from the age calculation of the mean without discussion of the selection criteria. Subsequent analysis of Candiota tonstein A by SIMS yielded an age of 294.0 +3.8/-4.2 Ma (2σ) using TuffZirc (Ludwig, 2008) (Fig. 1; Guerra-Sommer et al., 2008c), which included one discordant point. Two concordant grains are younger then the TuffZirc age.

Candiota C Upper Candiota 1 *(Locality 31°27’43.69”S 53°41’33.01”W*)

For the overlying Candiota C tonstein, an age of 296.9 ±1.6 Ma was calculated from the weighted mean of five multi-crystal analyses measured by TIMS (Fig. 1 and 2; Guerra-Sommer 2008a). Two of the five grains were discordant and were incorrectly used in calculation of a weighted mean age. Tonstein C was reanalyzed by SIMS and an age of 289.4 +1.8/-1.6 Ma was reported using TuffZirc (Fig. 1; Guerra-Sommer et al., 2008c).

Hulha Negra Candiota (HNC-C4) *(Locality 31°23’41.50”S 53°47’16.12”W)*

Mori et al. (2012) sampled a tonstein deposit that is ~15 m above the Candiota A tonstein from outcrop (Fig. 3) and analyzed isolated zircons by LA-ICP-MS. The age inventory for the analysis is complex with 3 age components identified. The oldest age component ($^{207}Pb/^{206}Pb$ age >1.5 Ga) was interpreted as inherited. The remaining two age components have distinct concordia ages of 281.4 ±3.4 Ma (1σ) and 295.4 ±4.5 Ma (1σ). The authors interpret the 281.4 ±3.4 Ma age as the depositional age and suggest the zircons used to calculate the 295.4 ±4.5 Ma age were inherited. The grains selected to calculate the youngest (281.4 ±3.4 Ma) and the older (295.4 ±4.5 Ma) age components were chosen based on their Th/U ratios that varied from 0.33-0.92 for the youngest to 2.03-4.74 for the oldest age component. A single low Th/U (0.35) grain with a 302 Ma age ($^{206}Pb/^{238}U$) and an elevated Th/U grain with a 274 Ma age were not used in the calculation of the low and high Th/U ages, suggesting subjective age selection criteria. Two biozones were recorded through the exposure of this outcrop, named as *Vittatina costabilis* (VCIZ) and *Lueckisporites virrkiae* (LVIZ) interval zones (Fig. 4). The depositional age assumed by Mori et al. (2012) permitted to consider this as the oldest occurrence of the LVIZ in Paraná Basin.

Faxinal Coal *(Locality 30°15’58.22"S 51°42’13.36"W)*

A weighted mean age of 285.4 ±8.6 Ma (MSWD = 7.1; σ not specified) was reported from 4 multi-crystal batch analyses measured by TIMS (Fig 1). Only one sample out of four is concordant (if the decay constant uncertainty is taken into consideration). Guerra-Sommer et al. (2008c) re-analyzed this sample by ion microprobe and calculated a TuffZirc age of 290.2 +2.5/-0.9 (2σ) Ma (Fig. 1). Two of eighteen zircons included in the age calculation are discordant.

The overlap in the uncertainty of published ages for the Candiota Coal interval in the Rio Bonito Fm has been argued for synchroneity of the coal deposits across the southern Paraná Basin (Fig. 1; Guerra-Sommer et al., 2008c; Simas et al., 2012). The correlation of the coals is problematic based on the published stratigraphic framework as the age of the Hulha Negra Candiota tonstein is several Myr younger, outside the uncertainty, of the Candiota and Faxinal ages despite its stratigraphic proximity (~15m) to the Candiota A tonstein. The palynological assemblages from Faxinal Coal are referred to the *Vittatina costabilis* Interval Zone (VCIZ) (Fig. 4; Guerra-Sommer et al., 2008a,b) despite the occurrence of *Lueckisporites virkkiae*, the key taxon for the overlying *L. virkkiae* Interval Zone (LVIZ) (Fig. 4; Boardman et al., 2012).

Quitéria *(Locality 30°20’16.90”S 52°10’14.50”W)*

Lastly, the palynological-based biostratigraphy for southwestern Gondwana (Mori et al., 2012; Césari et al., 2011) used for correlation of the Paraná succession throughout

Gondwana solely relies on the aforementioned radioisotopic ages. The palynological assemblages within a key outcrop (Quiteria) suggest that deposition of the Rio Bonito Fm continued throughout the early Permian (Kungarian Stage, 279.3-272.3 Ma) (Fig. 4; Jasper et al., 2006; Boardman et al., 2012).

Analytical procedures

Single zircon U-Pb analyses were performed at the Berkeley Geochronology Center. The volcaniclastic samples and mineral concentrates were then purified using standard mineral separation techniques, including sieves, magnetic separation and density separation. Euhedral, clear grains devoid of optically recognizable cores were chosen for analysis although older cryptic cores often escape detection in transmitted light (the results from most samples analyzed in this study suggest that small old cores are present in many cases). All zircons were pretreated using thermal annealing at 850°C for 48 hrs, followed by chemical abrasion (Mattinson, 2005) with concentrated HF in pressurized dissolution capsules at 220°C for 6-8 hrs. Prior to dissolution the crystals were cleaned in ultrasonically agitated aqua regia followed by multiple steps of rinsing in clean HNO3. Zircon crystals were then spiked with ^{205}Pb-^{233}U-^{235}U tracer solution and dissolved by vapor transfer in HF using miniature PTFE capsules at 220°C for 6 days. After dissolution, large crystals where loaded in 2 to 3 aliquots (see table) to optimize beam stability (which typically is significantly decreased for large, unextracted zircon samples) and test reproducibility. Isotope ratios were determined on a Micromass Sector 54 mass spectrometer using a Daly-type ion counter positioned behind a WARP filter. Pb (as Pb^{+}) and U (as UO^{2+}) were run sequentially on the same filament. The accuracy of the used mixed tracer was tested repeatedly against solutions derived from certified standards of isotopically pure ^{206}Pb and natural U (NIST SRM-991 and CRM-145, respectively), as well as age solutions distributed by the Earthtime initiative (agreement was found to be <0.1%, additional details regarding tracer calibration are in Irmis et al., 2011; Mundil et al., 2004; Black et al., 2004). In addition, 6 single zircons from the Quitéria sample were analyzed against the EarthTime 535 (ET 535) tracer solution, which was made available after the ages presented in this contribution were generated. The results from this batch are in agreement with the ones obtained using the BGC tracer solution, and discussed together with the previous Quiteria data. Repeat measurements of the total procedural blank averaged 0.82 ± 0.36 pg Pb (U blanks were indistinguishable from zero), with ^{206}Pb/^{204}Pb = 18.40 ± 0.46, ^{207}Pb/^{204}Pb = 15.64 ± 0.25, ^{208}Pb/^{204}Pb = 38.04 ± 0.75 (all 2σ of population), and a ^{206}Pb/^{204}Pb-^{207}Pb/^{204} Pb correlation of +0.47 (ratios and uncertainties were propagated into the age and age-error calculations). The common Pb composition was tested using a total 3-D isochron (Ludwig, 1998) for data sets that displayed coherent concordant clusters in Wetherill Concordia plots (QUI, CT3). Common Pb plane intercepts were found to be at ^{206}Pb/^{204}Pb = 18.20 ± 0.21, ^{207}Pb/^{204}Pb = 15.640 ± 0.047, error correl. = +0.46 (for QUI), and ^{206}Pb/^{204}Pb = 18.45 ± 0.80, ^{207}Pb/^{204}Pb = 15.659 ± 0.068, error correl. = +0.716 (for CT3). Calculated and measured common Pb composition is in good agreement suggesting that the common Pb composition applied to Pb analyses is reasonable. Total 3-D isochron ages for these samples are in agreement with weighted mean ^{206}Pb/^{238}U ages. The total procedural blank including ion exchange chemistry at BGC is also as low as 1 pg but scatter in total common Pb concentration and possibly common Pb composition suggests that results from unextracted analyses of zircon yield better reproducibility. Since the analysis of large unextracted zircon crystals results in unstable ion beams, large sample were split into aliquots (only for Faxinal samples). Deficient radiogenic ^{206}Pb in zircon due to initial deficit of ^{230}Th is accounted for by assuming a partition coefficient ratio DTh/DU of 0.2 (as applied in Wotzlaw et al., 2014). Mass fractionation of U during analysis was controlled by the U double spike, whereas Pb mass fractionation was corrected by 0.15 ± 0.6 %/AMU (based on multiple analyses of NBS 981).

References:

Black, L.P., Kamo, S.L., Allen, C.M., Davis, D.W., Aleinikoff, J.N., Valley, J.W., Mundil, R., Campbell, I.H., Korsch, R.J., Williams, I.S., and Foudoulis, C., 2004, Improved 206Pb/238U microprobe geochronology by the monitoring of a trace-element-related matrix effect; SHRIMP, ID-TIMS, ELA-ICP-MS and oxygen isotope documentation for a series of zircon standards: Chemical Geology, v. 205, p. 115-140.

Boardman, D. R., Souza, P. A., Iannuzzi, R., and Mori, A. L. O., 2012, Paleobotany and Palynology of the Rio Bonito Formation (Lower Permian, Parana Basin, Brazil) at the Quitéria Outcrop: Ameghiniana, v. 49, no. 4, p. 451-472.

Césari, S. N., Limarino, C. O., and Gulbranson, E. L., 2011, An Upper Paleozoic bio-chronostratigraphic scheme for the western margin of Gondwana: Earth-Science Reviews, v. 106, no. 1, p. 149-160.

de Matos, S. L. F., Yamamoto, J. K., Riccomini, C., Hachiro, J., and Tassinari, C. C. G., 2001, Absolute dating of Permian ash-fall in the Rio Bonito formation, Paraná Basin, Brazil: Gondwana Research, v. 4, no. 3, p. 421-426.

Guerra-Sommer, M., Cazzulo-Klepzig, M., Santos, J. O. S., Hartmann, L. A., Ketzer, J. M., and Formoso, M. L. L., 2008a, Radiometric age determination of tonsteins and stratigraphic constraints for the Lower Permian coal succession in southern Parana Basin, Brazil: International Journal of Coal Geology, v. 74, no. 1, p. 13-27. doi:10.1016/j.coal.2007.09.005.

Guerra-Sommer, M., Cazzulo-Klepzig, M., Menegat, R., Laquintinie Formoso, M. L., Stipp Basei, M. A., Barboza, E. G., and Simas, M. W., 2008b, Geochronological data from the Faxinal coal succession, southern Parana Basin, Brazil: A preliminary approach combining radiometric U-Pb dating and palynostratigraphy: Journal of South American Earth Sciences, v. 25, no. 2, p. 246-256. doi:10.1016/j.jsames.2007.06.007.

Guerra-Sommer, M., Cazzulo-Klepzig, M., Laquintinie Formoso, M. L., Menegat, R., and Mendonca Fo, J. G., 2008c, U-Pb dating of tonstein layers from a coal succession of the southern Parana Basin (Brazil): A new geochronological approach: Gondwana Research, v. 14, no. 3, p. 474-482. doi:10.1016/j.gr.2008.03.003.

Irmis, R.B., Mundil, R., Martz, J.W., and Parker, W.G., 2011, High-resolution U–Pb ages from the Upper Triassic Chinle Formation (New Mexico, USA) support a diachronous rise of dinosaurs: Earth and Planetary Science Letters, v. 309, p. 258-267.

Jasper, A., Menegat, R., Guerra-Sommer, M., Cazzulo-Klepzig, M., and de Souza, P. A., 2006, Depositional cyclicity and paleoecological variability in an outcrop of Rio Bonito formation, Early Permian, Paraná Basin, Rio Grande do Sul, Brazil: Journal of South American Earth Sciences, v. 21, no. 3, p. 276-293.

Ludwig, K.R., 1998, On the treatment of concordant uranium-lead ages: Geochimica et Cosmochimica Acta, v. 62, p. 665-676.

Mattinson, J.M., 2005, Zircon U-Pb chemical abrasion ("CA-TIMS") method: Combined annealing and multi-step partial dissolution analysis for improved precision and accuracy of zircon ages: Chemical Geology, v. 220, p. 47-66.

Mori, A. L.O., de Souza, P. A., Marques, J. C., and Lopes, R. d. C., 2012, A new U-Pb zircon age dating and palynological data from a Lower Permian section of the southernmost Parana Basin, Brazil: Biochronostratigraphical and geochronological implications for Gondwanan correlations: Gondwana Research, v. 21, no. 2-3, p. 654-669. doi:10.1016/j.gr.2011.05.019.

Mundil, R., Ludwig, K.R., Metcalfe, I., and Renne, P.R., 2004, Age and timing of the Permian mass extinctions: U/Pb dating of closed-system zircons: Science, v. 305, p. 1760-1763.

Wotzlaw, J.-F., Hüsing, S.K., Hilgen, F.J., and Schaltegger, U., 2014, High-precision zircon U–Pb geochronology of astronomically dated volcanic ash beds from the Mediterranean Miocene: Earth and Planetary Science Letters, v. 407, p. 19-34.

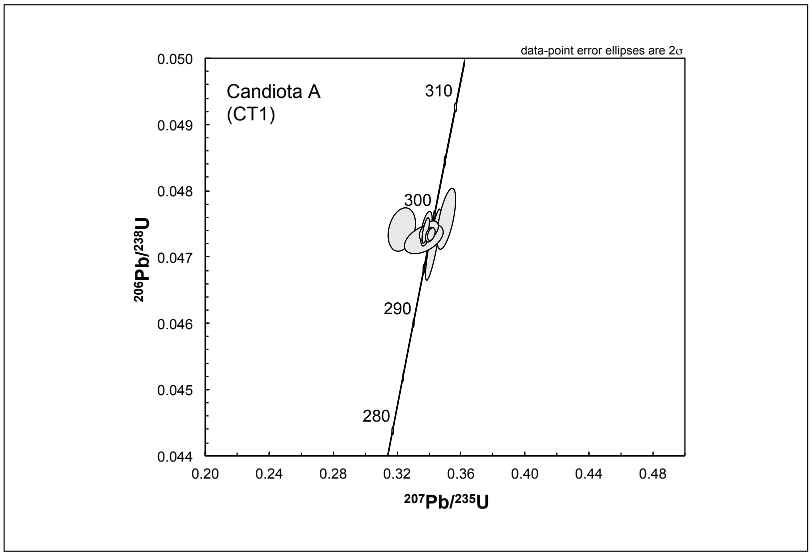
data-point error ellipses are 2σ
Candiota A
(CT1)
310
300
290
280
0.050
0.049
0.048
0.047
0.046
0.045
0.044
0.20
0.24
0.28
0.32
0.36
0.40
0.44
0.48
206Pb/238U
207Pb/235U

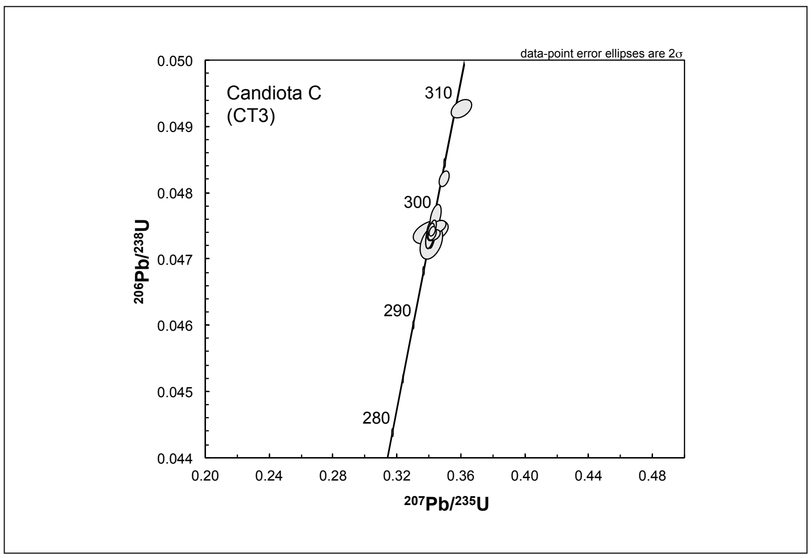
data-point error ellipses are 2σ
Candiota C
(CT3)
310
300
290
280
0.050
0.049
0.048
0.047
0.046
0.045
0.044
0.20
0.24
0.28
0.32
0.36
0.40
0.44
0.48
206Pb/238U
207Pb/235U

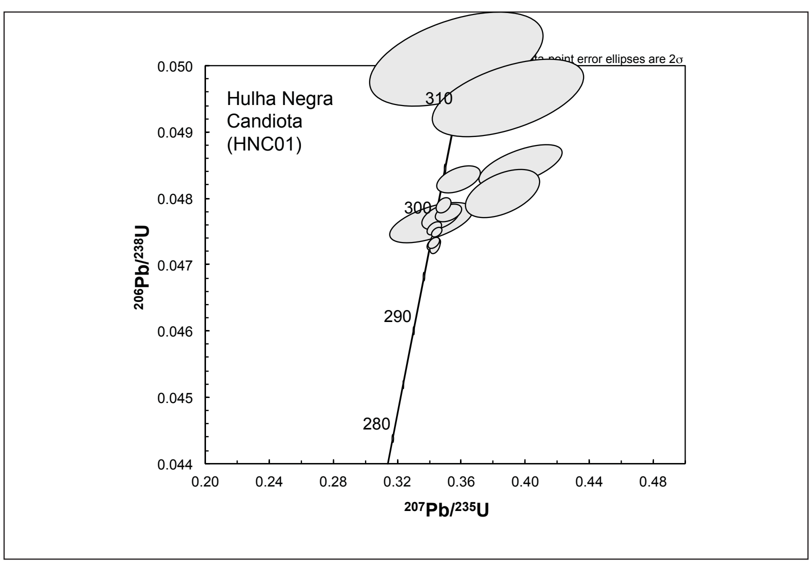
Hulha Negra
Candiota
(HNC01)
310
300
290
280
0.050
0.049
0.048
0.047
0.046
0.045
0.044
0.20
0.24
0.28
0.32
0.36
0.40
0.44
0.48
206Pb/238U
207Pb/235U

191

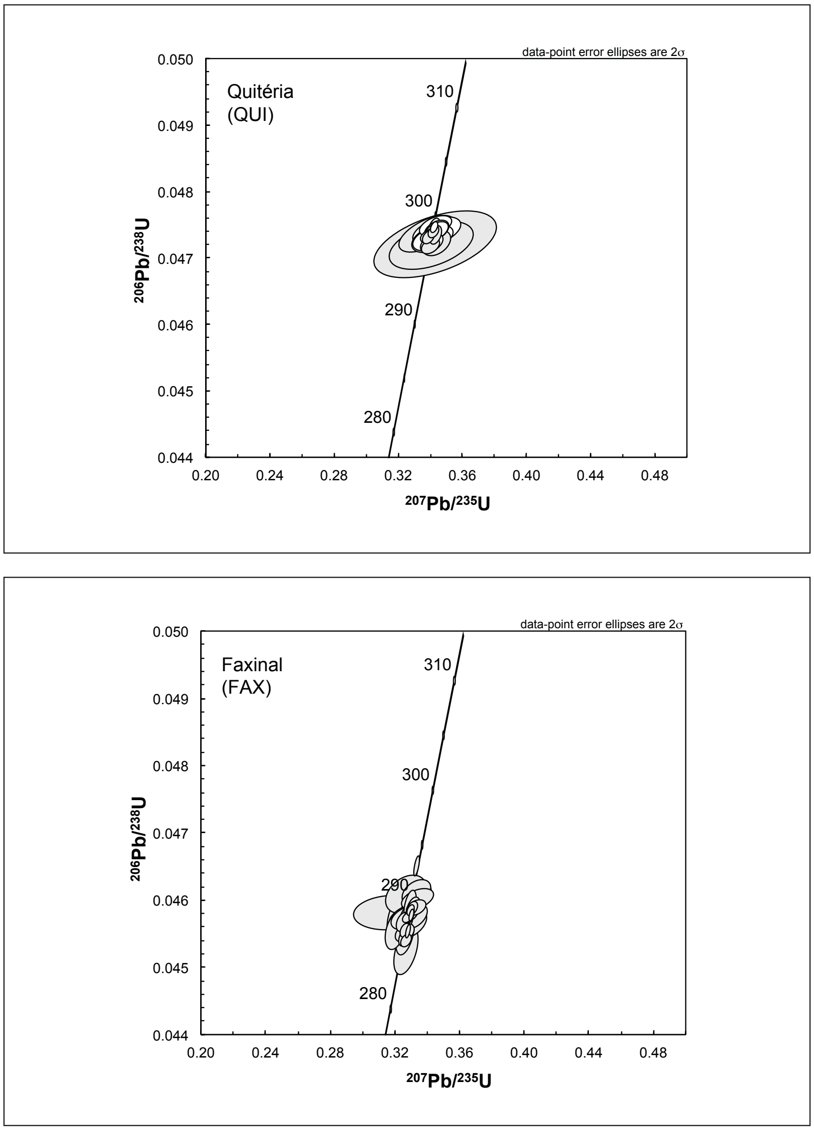

Supplementary Fig. 1. Concordia plots for all volcaniclastic samples presented in this study. Error ellipses are two-sigma and filled (gray). White ellipses (Quitéria) are spiked with EarthTime 535 Tracer.

Table DR1			isotopic ratios								isotopic age in (Ma)	
Sample	Pb_c (pg)	$\frac{Th}{U}$	$\frac{^{206}Pb}{^{204}Pb}$	$\frac{^{207}Pb}{^{206}Pb}$	2σ %er	$\frac{^{207}Pb}{^{235}U}$	2σ %er	$\frac{^{206}Pb}{^{238}U}$	2σ %er	ρ	$\frac{^{206}Pb^*}{^{238}U}$	
FAX.Z001	2.0	0.50	1616	0.05189	1.03	0.3270	1.13	0.045711	0.40	.43	288.14	± 1.15
FAX.Z002	0.6	0.79	1041	0.05100	1.47	0.3203	1.57	0.045546	0.49	.35	287.12	± 1.40
FAX.Z003	0.7	0.55	886	0.05204	0.55	0.3285	0.60	0.045785	0.16	.41	288.59	± 0.47
FAX.Z004	0.5	0.61	762	0.05196	0.71	0.3264	0.77	0.045564	0.19	.38	287.23	± 0.53
FAX.Z006	0.5	0.66	2574	0.05208	0.82	0.3298	0.93	0.045927	0.41	.47	289.47	± 1.18
FAX.Z007	0.8	0.59	1179	0.05187	0.62	0.3264	0.72	0.045629	0.32	.51	287.63	± 0.92
FAX.Z008	0.6	0.68	4906	0.05189	0.32	0.3274	0.55	0.045757	0.43	.81	288.42	± 1.25
FAX.Z31.1	0.7	0.60	627	0.05205	1.25	0.3265	1.41	0.045492	0.53	.47	286.78	± 1.53
FAX.Z31.2	0.6	0.60	671	0.05223	0.75	0.3270	0.79	0.045409	0.17	.38	286.27	± 0.48
FAX.Z31.3	1.2	0.60	360	0.05198	1.42	0.3263	1.49	0.045523	0.24	.39	286.98	± 0.68
FAX.Z31.4	0.5	0.60	759	0.05196	0.72	0.3256	0.78	0.045451	0.22	.40	286.53	± 0.64
FAX.Z31											286.52	± 0.32
FAX.Z32.1	2.5	0.48	247	0.05255	2.01	0.3338	2.13	0.046071	0.39	.38	290.35	± 1.13
FAX.Z32.2	2.9	0.48	215	0.05268	2.34	0.3343	2.44	0.046023	0.28	.43	290.06	± 0.80
FAX.Z32.3	2.6	0.46	238	0.05146	3.00	0.3271	3.13	0.046096	0.50	.35	290.51	± 1.45
FAX.Z32.4	2.6	0.47	241	0.05244	2.08	0.3335	2.19	0.046124	0.33	.39	290.68	± 0.97
FAX.Z32											290.34	± 0.50
FAX.Z34.1	0.4	0.37	1008	0.05219	0.51	0.3300	0.56	0.045861	0.14	.41	289.06	± 0.42
FAX.Z34.2	0.6	0.37	638	0.05153	2.32	0.3249	2.45	0.045730	0.75	.33	288.25	± 2.15
FAX.Z34.3	0.8	0.37	461	0.05016	5.70	0.3169	5.73	0.045823	0.45	.11	288.83	± 1.30
FAX.Z34											289.01	± 0.38
FAX.Z35.1	1.5	0.59	289	0.05229	1.85	0.3302	1.99	0.045803	0.50	.40	288.70	± 1.46
FAX.Z35.2	2.0	0.59	210	0.05194	2.67	0.3277	2.81	0.045755	0.34	.44	288.41	± 0.99
FAX.Z35.3	1.8	0.59	241	0.05234	2.42	0.3295	2.56	0.045662	0.39	.42	287.83	± 1.12
FAX.Z35.4	1.9	0.59	222	0.05206	2.51	0.3284	2.62	0.045747	0.32	.39	288.36	± 0.93
FAX.Z35											288.30	± 0.53
FAX.Z36.1	0.3	0.67	2069	0.05225	0.41	0.3302	0.46	0.045831	0.18	.44	288.87	± 0.51
FAX.Z36.2	0.8	0.67	718	0.05230	0.75	0.3309	0.81	0.045888	0.18	.40	289.23	± 0.52
FAX.Z36.3	1.4	0.67	423	0.05267	1.39	0.3333	1.46	0.045899	0.20	.38	289.29	± 0.58
FAX.Z36											289.12	± 0.30
FAX.Z38.1	0.4	0.66	1027	0.05160	0.95	0.3250	1.02	0.045685	0.25	.39	287.97	± 0.71
FAX.Z38.2	0.5	0.67	776	0.05196	0.69	0.3277	0.73	0.045750	0.13	.37	288.37	± 0.36
FAX.Z38.3	1.0	0.67	390	0.05267	1.79	0.3324	1.91	0.045769	0.32	.44	288.49	± 0.93
FAX.Z38											288.31	± 0.30
FAX.Z39.1	0.4	0.53	1803	0.05233	0.32	0.3304	0.37	0.045785	0.15	.51	288.59	± 0.44
FAX.Z39.2	0.9	0.53	748	0.05214	0.64	0.3289	0.69	0.045748	0.14	.38	288.36	± 0.40
FAX.Z39											288.47	± 0.29
FAX.301	0.7	0.66	4720	0.05202	0.32	0.3336	0.43	0.046515	0.26	.66	293.09	± 0.77
FAX.302	0.8	0.79	469	0.05241	1.66	0.3271	1.86	0.045263	0.64	.47	285.37	± 1.84
FAX.303	0.8	0.82	623	0.05243	0.94	0.3317	1.03	0.045881	0.30	.42	289.19	± 0.87
FAX.305	0.8	0.76	2006	0.05227	0.30	0.3283	0.37	0.045548	0.18	.58	287.13	± 0.51
FAX.306	0.7	0.70	1246	0.05230	0.41	0.3303	0.49	0.045810	0.24	.55	288.74	± 0.68
FAX.307	0.8	0.83	1395	0.05217	0.42	0.3295	0.47	0.045807	0.17	.46	288.73	± 0.49
CT1.Z001	1.2	0.75	782	0.05168	0.72	0.3380	0.87	0.047432	0.45	.57	298.74	± 1.35
CT1.Z002	0.9	0.80	716	0.05339	1.03	0.3503	1.33	0.047586	0.79	.64	299.68	± 2.36
CT1.Z005	1.2	0.75	1171	0.05223	0.53	0.3410	0.58	0.047351	0.16	.40	298.24	± 0.48
CT1.Z006	1.4	0.79	1467	0.04930	2.12	0.3223	2.20	0.047421	0.57	.27	298.67	± 1.69
CT1.Z204	0.4	0.80	1839	0.05166	0.39	0.3377	0.53	0.047409	0.33	.67	298.59	± 0.99
CT1.Z205	0.7	0.88	973	0.05210	0.61	0.3401	0.67	0.047343	0.19	.41	298.19	± 0.58
CT1.Z206	0.5	0.83	2430	0.05260	0.60	0.3423	1.12	0.047193	0.92	.85	297.26	± 2.74
CT1.Z207	0.5	0.67	649	0.05193	1.40	0.3394	1.50	0.047400	0.26	.46	298.54	± 0.77
CT1.Z208	0.7	0.75	378	0.05159	2.78	0.3363	2.94	0.047282	0.38	.47	297.81	± 1.14
QUI.Z003	0.8	0.74	717	0.05225	0.79	0.3415	0.83	0.047401	0.15	.37	298.54	± 0.46
QUI.Z004	1.4	0.71	432	0.05223	1.21	0.3405	1.31	0.047287	0.36	.40	297.85	± 1.06
QUI.Z005	0.7	0.69	724	0.05187	0.82	0.3384	0.87	0.047319	0.17	.38	298.04	± 0.50
QUI.Z006	1.1	0.69	704	0.05227	0.94	0.3415	1.05	0.047383	0.38	.45	298.44	± 1.13
QUI.Z207	1.6	0.65	432	0.05223	1.27	0.3398	1.34	0.047185	0.20	.41	297.22	± 0.61
QUI.Z208	1.2	0.73	307	0.05254	1.76	0.3436	1.86	0.047423	0.26	.42	298.68	± 0.77
QUI.Z209	0.9	0.66	940	0.05253	0.82	0.3429	0.88	0.047351	0.24	.39	298.24	± 0.72
QUI.Z210	2.8	0.91	251	0.05276	2.01	0.3436	2.12	0.047227	0.33	.39	297.48	± 0.98
QUI.Z211	4.2	0.71	76	0.05266	8.71	0.3428	9.12	0.047209	0.87	.51	297.36	± 2.58
QUI.Z213	1.6	0.82	185	0.05220	2.85	0.3404	2.98	0.047292	0.35	.42	297.87	± 1.05
QUI.Z216	1.5	0.76	363	0.05211	1.48	0.3402	1.55	0.047344	0.19	.43	298.19	± 0.56
QUI.Z217	1.7	0.83	137	0.05228	6.11	0.3402	6.37	0.047195	0.62	.46	297.28	± 1.84
QUI.Z218	1.1	0.76	516	0.05168	3.98	0.3375	4.25	0.047370	0.48	.59	298.35	± 1.43
QUI.Z21*	1.4	0.53	328	0.05234	1.58	0.3407	1.67	0.047228	0.24	.44	297.39	± 0.71
QUI.Z22*	4.8	0.69	330	0.05258	1.66	0.3436	1.77	0.047408	0.24	.48	298.51	± 0.71
QUI.Z23*	1.3	0.76	1103	0.05228	0.52	0.3421	0.57	0.047469	0.14	.45	298.88	± 0.40
QUI.Z24*	4.3	0.75	181	0.05235	2.88	0.3413	3.02	0.047303	0.33	.47	297.86	± 0.95
QUI.Z25*	2.4	0.73	163	0.05261	3.39	0.3437	3.55	0.047407	0.37	.47	298.50	± 1.09
QUI.Z26*	2.1	0.93	238	0.05240	2.27	0.3429	2.38	0.047488	0.26	.47	299.01	± 0.77
HNC01.Z01	0.9	4.09	1281	0.05266	0.69	0.3433	0.74	0.047282	0.19	.41	297.82	± 0.56
HNC01.Z02	0.5	5.77	552	0.05279	1.01	0.3486	1.07	0.047896	0.20	.37	301.59	± 0.59
HNC01.Z03	0.9	2.85	137	0.05933	5.05	0.3967	5.37	0.048494	0.54	.63	305.27	± 1.64
HNC01.Z04	1.1	3.07	499	0.05250	0.97	0.3425	1.02	0.047312	0.16	.39	298.00	± 0.48
HNC01.Z05	0.5	3.79	149	0.05191	5.90	0.3409	6.19	0.047635	0.52	.59	299.98	± 1.56
HNC01.Z06	0.8	3.57	1072	0.05246	0.52	0.3424	0.58	0.047339	0.23	.47	298.16	± 0.69
HNC01.Z08	0.5	5.58	194	0.05377	2.99	0.3580	3.14	0.048288	0.34	.48	304.00	± 1.04
HNC01.Z09	0.8	4.40	66	0.04979	11.94	0.3567	12.45	0.051950	1.12	.49	326.48	± 3.65
HNC01.Z10	0.5	4.91	133	0.05817	4.66	0.3856	4.93	0.048078	0.61	.49	302.71	± 1.86

HNC01.Z11	1.1	2.04	1238	0.07547	0.37	0.6854	0.48	0.065866	0.26	.62	411.20	± 1.09
HNC01.Z12	0.8	4.24	74	0.05698	9.44	0.3890	9.93	0.049516	0.96	.54	311.55	± 3.00
HNC01.Z21	0.4	0.85	961	0.05260	0.74	0.3445	0.79	0.047495	0.12	.45	299.12	± 0.36
HNC01.Z22	0.4	7.75	279	0.05272	2.67	0.3469	2.81	0.047725	0.33	.48	300.54	± 0.99
HNC01.Z23	0.2	0.68	2079	0.05847	0.44	0.6985	0.49	0.086651	0.18	.44	535.70	± 0.97
HNC01.Z24	0.5	5.63	283	0.05339	1.82	0.3517	1.91	0.047784	0.23	.42	300.90	± 0.69
HNC01.Z25	0.4	5.61	984	0.05249	0.81	0.3426	0.87	0.047334	0.14	.46	298.13	± 0.43
HNC01.Z26	0.5	3.13	800	0.05228	1.04	0.3428	1.11	0.047553	0.17	.48	299.48	± 0.51
CT3.Z05	2.3	0.54	419	0.05300	1.36	0.3601	1.44	0.049269	0.23	.42	310.03	± 0.71
CT3.Z31	0.7	0.53	757	0.05251	0.71	0.3491	0.77	0.048215	0.20	.41	303.55	± 0.60
CT3.Z33	1.2	0.59	798	0.05235	0.73	0.3439	0.83	0.047645	0.32	.47	300.05	± 0.95
CT3.Z32	0.6	0.50	444	0.05275	1.09	0.3454	1.15	0.047490	0.16	.40	299.10	± 0.48
CT3.Z04	1.0	0.56	1183	0.05226	0.47	0.3420	0.54	0.047466	0.22	.51	298.94	± 0.66
CT3.Z35	1.4	0.49	624	0.05227	0.87	0.3420	0.96	0.047454	0.31	.43	298.87	± 0.91
CT3.Z06	1.6	0.55	1258	0.05214	0.45	0.3411	0.50	0.047439	0.18	.44	298.78	± 0.54
CT3.Z03	0.8	0.67	1319	0.05228	0.42	0.3418	0.46	0.047424	0.13	.42	298.69	± 0.38
CT3.Z10	2.4	0.45	203	0.05214	2.51	0.3409	2.63	0.047412	0.31	.43	298.61	± 0.93
CT3.Z30	0.9	0.62	1276	0.05240	0.42	0.3425	0.60	0.047405	0.42	.72	298.57	± 1.24
CT3.Z02	1.0	0.56	939	0.05232	0.58	0.3418	0.63	0.047384	0.16	.39	298.44	± 0.47
CT3.Z201	1.0	0.80	891	0.05217	0.60	0.3408	0.72	0.047376	0.36	.56	298.39	± 1.09
CT3.Z01	1.0	0.80	892	0.05219	0.62	0.3409	0.74	0.047375	0.37	.54	298.38	± 1.10
CT3.Z34	0.9	0.54	613	0.05252	0.87	0.3430	0.91	0.047368	0.14	.35	298.34	± 0.41
CT3.Z09	2.7	0.66	318	0.05238	1.56	0.3412	1.67	0.047250	0.43	.39	297.61	± 1.28

Pb blank composition is $^{206}Pb/^{204}Pb$ = 18.40 ± 0.64, $^{207}Pb/^{204}Pb$ = 15.64 ± 0.25, $^{208}Pb/^{204}Pb$ = 38.04 ± 0.75, and a $^{206}Pb/^{204}Pb$–$^{207}Pb/^{204}Pb$ correlation of +0.47.
Present day Th/U ratio is calculated from radiogenic $^{208}Pb/^{206}Pb$ and age.
Isotopic ratios corrected for mass fractionation (0.15 ± 0.06%/amu), tracer contribution and common Pb contribution (the latter for all ratios but $^{206}Pb/^{204}Pb$).
ρ is correlation coefficient of radiogenic $^{207}Pb/^{235}U$ versus $^{206}Pb/^{238}U$.
Analyses of aliquotes are printed in grey.
Uncertainties of individual ratios and ages are given at the 2σ level and do not include decay constant errors.
Samples denoted with an * were analyzed using the Earthtime 535 tracer solution.
Deficient radiogenic ^{206}Pb due to initial deficit of ^{230}Th is accounted for by assuming a partition coefficient ratio DTh/DU of 0.2 (as applied in Wotzlaw et al., 2014).
Initial deficit of ^{230}Th for zircons analyzed using ET535 is corrected assuming Th/U=3.5 in the magma.